Nonfactorizable charming-loop contribution to FCNC $B_s \to \gamma l^+ l^-$ decay

Ilia Belov,[1] Alexander Berezhnoy,[2] and Dmitri Melikhov[2,3,4]

[1]INFN, Sezione di Genova, via Dodecaneso 33, I-16146 Genova, Italy
[2]D. V. Skobeltsyn Institute of Nuclear Physics, M. V. Lomonosov Moscow State University, 119991, Moscow, Russia
[3]Joint Institute for Nuclear Research, 141980 Dubna, Russia
[4]Faculty of Physics, University of Vienna, Boltzmanngasse 5, A-1090 Vienna, Austria

(Received 1 April 2024; accepted 15 May 2024; published 10 June 2024)

We present the first theoretical calculation of nonfactorizable charm-quark loop contributions to the $B_s \to \gamma l^+ l^-$ amplitude. We calculate the relevant form factors, $H^{\rm NF}_{A,V}(k'^2, k^2)$, and provide convenient parametrizations of our results in the form of fit functions of two variables, k'^2 and k^2, applicable in the region below hadron resonances, $k'^2 < M^2_{J/\psi}$ and $k^2 < M^2_\phi$. We report that factorizable and nonfactorizable charm contributions to the $B_s \to \gamma l^+ l^-$ amplitude have opposite signs. To compare the charm and the top contributions, it is convenient to express nonfactorizable charming loop contribution as a nonuniversal (i.e., dependent on the reaction) q^2-dependent correction $\Delta^{\rm NF} C_7(q^2)$ to the Wilson coefficient C_7. For the $B_s \to \gamma l^+ l^-$ amplitude, the correction is found to be positive, $\Delta^{\rm NF} C_7(q^2)/C_7 > 0$.

DOI: 10.1103/PhysRevD.109.114012

I. INTRODUCTION

This paper reports the first theoretical analysis of nonfactorizable (NF) charming loops in rare flavor-changing neutral currents (FCNC) $B_s \to \gamma l^+ l^-$ decays making use of theoretical approach formulated in [1].

Charming loops in rare FCNC decays of the B-meson have visible impact on the B-decay observables [2] and their reliable theoretical description is necessary for studies of possible new physics effects (see, e.g., [3–12]).

A number of theoretical analyses of NF charming loops in FCNC B-decays has been published in the recent years: In [13], an effective gluon-photon local operator describing the charm-quark loop has been calculated as an expansion in inverse charm-quark mass m_c and applied to inclusive $B \to X_s\gamma$ decays (see also [14,15]); in [16], NF corrections in $B \to K^*\gamma$ using local operator product expansion (OPE) have been studied; NF corrections induced by a local photon-gluon operator have been calculated in [17,18] in terms of the light cone (LC) 3-particle antiquark-quark-gluon Bethe-Salpeter amplitude (3BS) of K^*-meson [19–21] with two field operators having equal coordinates, $\langle 0|\bar{s}(0)G_{\mu\nu}(0)u(x)|K^*(p)\rangle, x^2 = 0$. As noticed already long ago, local OPE for the charm-quark loop in FCNC B-decays leads to a power series in $\Lambda_{\rm QCD} m_b/m_c^2 \simeq 1$. To sum up numerically large $O(\Lambda_{\rm QCD} m_b/m_c^2)^n$ corrections, Ref. [22] obtained a nonlocal photon-gluon operator describing the charm-quark loop and evaluated its effect making use of 3BS of the B-meson in a collinear LC configuration $\langle 0|\bar{s}(x)G_{\mu\nu}(ux)b(0)|\bar{B}_s(p)\rangle$, $x^2 = 0$ [23,24]. The same collinear approximation (known to provide the dominant 3BS contribution to meson tree-level form factors [25,26]) was applied also to the analysis of other FCNC B-decays [27].

In later publications [28–31], it was proven that the dominant contribution to FCNC B-decay amplitudes is actually given by the convolution of a hard kernel with the 3BS in a different configuration; a double-collinear light cone configuration $\langle 0|\bar{s}(y)G_{\mu\nu}(x)b(0)|\bar{B}_s(p)\rangle$, where $y^2 = 0$, $x^2 = 0$, but $xy \neq 0$. The corresponding factorization formula was derived in [31]. The first application of a double-collinear 3BS to FCNC $B_s \to \gamma\gamma$ decays was presented in [32,33].

As a further step, [1] developed a theoretical approach to NF charming loops in FCNC B-decays based on a generic 3BS of the B-meson. This approach makes use of rigorous properties of the generic 3BS: Namely, the generic 3BS of the B-meson contains new Lorentz structures (compared to the collinear and the double-collinear configurations) and new three-particle distribution amplitudes (3DAs) that appear as the coefficients multiplying these Lorentz structures; analyticity and continuity of the 3BS as the function of its arguments at the point $xp = yp = x^2 = y^2 = 0$ leads to certain constraints on the 3DAs [31] which were implemented in the 3BS model of [1]. Moreover, [1] applied this approach to $B_s \to \gamma\gamma$ decays.

Here we extend the analysis of [1] to the case of $B_s \to \gamma l^+ l^-$ decays. The paper is organized as follows. Section II recalls general formulas for the top contribution to the $B_s \to \gamma l^+ l^-$ amplitude and describes the connection between the charm contribution to the amplitudes of $B_s \to \gamma l^+ l^-$ and $B_s \to \gamma^* \gamma^*$ containing two virtual photons in the final state, including constraints on the latter imposed by electromagnetic gauge invariance. Section III outlines the calculation of the factorizable and nonfactorizable charming-loop contributions to the $B_s \to \gamma^* \gamma^*$ amplitude. Section IV gives numerical predictions for the form factors $H^{\rm NF}_{A,V}(k'^2, k^2)$ describing NF charm in $B_s \to \gamma^* \gamma^*$ decays and compares charm contributions with those of the top quark. Section V presents our concluding remarks. Appendixes A and B summarize some necessary details of our theoretical analysis. Appendixes C and D contain convenient and simple fit formulas for the form factors $H^{\rm NF}_{A,V}(k'^2, k^2)$ and $F_{TV,TA}(k'^2, k^2)$ in a broad range of their arguments k'^2 and k^2.

II. TOP AND CHARM CONTRIBUTIONS TO $B_s \to \gamma l^+ l^-$ AMPLITUDE

A standard theoretical framework for the description of the FCNC $b \to s$ transitions is provided by the Wilson OPE; the $b \to s$ effective Hamiltonian describing dynamics at the scale μ, appropriate for B-decays, reads [34–36] (we use the sign convention for the effective Hamiltonian and the Wilson coefficients adopted in [37,38]),

$$H^{b\to s}_{\rm eff} = \frac{G_F}{\sqrt{2}} V_{tb} V^*_{ts} \sum_i C_i(\mu) \mathcal{O}^{b\to q}_i(\mu), \tag{2.1}$$

G_F is the Fermi constant. The basis operators $\mathcal{O}^{b\to q}_i(\mu)$ contain only light degrees of freedom (u, d, s, c, and b-quarks, leptons, photons, and gluons); the heavy degrees of freedom of the SM (W, Z, and t-quark) are integrated out and their contributions are encoded in the Wilson coefficients $C_i(\mu)$. The light degrees of freedom remain dynamical and the corresponding diagrams containing these particles in the loops—in our case virtual c and u quarks—should be calculated and added to the diagrams generated by the effective Hamiltonian. For the SM Wilson coefficients at the scale $\mu_0 = 5$ GeV (the corresponding operators are listed below) we use the recent determination [corresponding to $C_2(M_W) = -1$] from [39]: $C_1(\mu_0) = 0.147$, $C_2(\mu_0) = -1.053$, $C_7(\mu_0) = 0.330$, $C_9(\mu_0) = -4.327$, $C_{10}(\mu_0) = 4.262$.

A. Top-quark contribution

Top-quark contribution to the $\bar{B}_s \to \gamma l^+ l^-$ amplitude is defined as follows [40]:

$$A^{(\bar{B}_s\to\gamma ll)}_{\rm top} = \langle \gamma(q') l^+(p_1) l^-(p_2) | H^{b\to s}_{\rm eff} | \bar{B}_s(p) \rangle, \quad q = p_1 + p_2. \tag{2.2}$$

Necessary for the $\bar{B}_s \to \gamma l^+ l^-$ decays of interest are the following terms in (2.1),[1]

$$\begin{aligned} H^{b\to s l^+ l^-}_{\rm eff} = {} & \frac{G_F}{\sqrt{2}} \frac{\alpha_{\rm em}}{2\pi} V_{tb} V^*_{ts} \\ & \times \left[-2 i m_b \frac{C_7(\mu)}{q^2} \cdot \bar{s} \sigma_{\mu\nu} q^\nu (1+\gamma_5) b \cdot \bar{l} \gamma^\mu l \right. \\ & + C_9(\mu) \cdot \bar{s} \gamma_\mu (1-\gamma_5) b \cdot \bar{l} \gamma^\mu l \\ & \left. + C_{10}(\mu) \cdot \bar{s} \gamma_\mu (1-\gamma_5) b \cdot \bar{l} \gamma^\mu \gamma_5 l \right]. \end{aligned} \tag{2.3}$$

The C_7 part of $H^{b\to s l^+ l^-}_{\rm eff}$ is obtained from

$$\begin{aligned} H^{b\to s\gamma}_{\rm eff} &= -\frac{G_F}{\sqrt{2}} V_{tb} V^*_{ts} C_7(\mu) \frac{e}{8\pi^2} m_b \cdot \bar{s} \sigma_{\mu\nu} (1+\gamma_5) b \cdot F^{\mu\nu} \\ &= \frac{G_F}{\sqrt{2}} V_{tb} V^*_{ts} C_7(\mu) \frac{e}{8\pi^2} 2 m_b i \cdot \bar{s} \sigma_{\mu\nu} q^\nu (1+\gamma_5) b \cdot \epsilon^\mu(q), \end{aligned} \tag{2.4}$$

by the replacement $\epsilon^\mu(q) \to \frac{1}{q^2} \bar{l} \gamma^\mu l e Q_l$, $Q_l = -1$, and corresponds to the diagram Fig. 1(a) with the virtual photon emitted from the penguin. Notice that the sign of the $b \to s\gamma$ effective Hamiltonian (2.4) correlates with the sign of the electromagnetic vertex. For a fermion with the electric charge $Q_q e$, we use in the Feynman diagrams the vertex

$$i Q_q e \bar{q} \gamma_\mu q \epsilon^\mu. \tag{2.5}$$

The $\bar{B}_s \to \gamma^*$ transition form factors of the basis operators in (2.3) are defined as [41]

$$\begin{aligned} \langle \gamma(k) | \bar{s} \gamma_\mu \gamma_5 b | \bar{B}_s(p) \rangle &= i e \varepsilon_\alpha(k) (g_{\mu\alpha} k'k - k'_\alpha k_\mu) \\ &\quad \times \frac{F_A(k'^2, k^2)}{M_{B_s}}, \\ \langle \gamma(k) | \bar{s} \gamma_\mu b | \bar{B}_s(p) \rangle &= e \varepsilon_\alpha(k) \epsilon_{\mu\alpha k' k} \frac{F_V(k'^2, k^2)}{M_{B_s}}, \\ \langle \gamma(k) | \bar{s} \sigma_{\mu\nu} \gamma_5 b | \bar{B}_s(p) \rangle k'^\nu &= e \varepsilon_\alpha(k) (g_{\mu\alpha} k'k - k'_\alpha k_\mu) \\ &\quad \times F_{TA}(k'^2, k^2), \\ \langle \gamma(k) | \bar{s} \sigma_{\mu\nu} b | \bar{B}_s(p) \rangle k'^\nu &= i e \varepsilon_\alpha(k) \epsilon_{\mu\alpha k' k} F_{TV}(k'^2, k^2). \end{aligned} \tag{2.6}$$

[1] Our notations and conventions are $\gamma^5 = i\gamma^0\gamma^1\gamma^2\gamma^3$, $\sigma_{\mu\nu} = \frac{i}{2}[\gamma_\mu, \gamma_\nu]$, $\epsilon^{0123} = -1$, $\epsilon_{abcd} \equiv \epsilon_{\alpha\beta\mu\nu} a^\alpha b^\beta c^\mu d^\nu$, $e = \sqrt{4\pi\alpha_{\rm em}}$.

We treat the form factors as functions of two variables, $F_i(k'^2, k^2)$; here k' is the momentum emitted from the FCNC $b \to s$ vertex, and k is the momentum of the (virtual) photon emitted from the valence quark of the B-meson, $p = k + k'$. The constraints on the form factors imposed by gauge invariance are discussed in Appendix A. Notice that the amplitude of the operator $\bar{s}\sigma_{\mu\nu}bk'^{\nu}$ is reduced to a single Lorentz structure and one form factor $F_{TA}(k'^2, k^2)$ if $k^2 = 0$ or $k'^2 = 0$.

1. Direct emission of the real photon from valence quarks of the B-meson

We denote as $A^{(1)}_{\rm top}$ the contribution to the $\bar{B}_s \to \gamma l^+ l^-$ amplitude, induced by $H^{b\to s l^+ l^-}_{\rm eff}$; the real photon is directly emitted from the valence s or b quark, and the $l^+ l^-$ pair is coupled to the FCNC vertex, Figs. 1(a) and 1(b). It corresponds to the momenta $k' = q$, $k = p - q$, $k'^2 = q^2$, and $k^2 = 0$, and thus involves the form factors $F_i(q^2, 0)$ [42],

$$\begin{aligned} A^{(1)}_{\rm top} &= \langle \gamma(k), l^+(p_1), l^-(p_2)|H^{b\to s l^+ l^-}_{\rm eff}|\bar{B}_s(p)\rangle \\ &= \frac{G_F}{\sqrt{2}} V_{tb}V^*_{ts}\frac{\alpha_{\rm em}}{2\pi} e\varepsilon_\alpha(k)[\epsilon_{\mu\alpha k' k}A^{(1)}_V(q^2)\bar{l}(p_2)\gamma_\mu l(-p_1) - i(g_{\mu\alpha}k'k - k'_\alpha k_\mu)A^{(1)}_A(q^2)\bar{l}(p_2)\gamma_\mu l(-p_1) \\ &\quad + \epsilon_{\mu\alpha k' k}A^{(1)}_{5V}(q^2)\bar{l}(p_2)\gamma_\mu\gamma_5 l(-p_1) - i(g_{\mu\alpha}k'k - k'_\alpha k_\mu)A^{(1)}_{5A}(q^2)\bar{l}(p_2)\gamma_\mu\gamma_5 l(-p_1)], \qquad k' = q, \quad k = p - q, \end{aligned} \tag{2.7}$$

with

$$\begin{aligned} A^{(1)}_{V(A)}(q^2) &= \frac{2C_7(\mu)}{q^2} m_b F_{TV(TA)}(q^2, 0) \\ &\quad + C_9(\mu)\frac{F_{V(A)}(q^2, 0)}{M_B}, \\ A^{(1)}_{5V(5A)}(q^2) &= C_{10}(\mu)\frac{F_{V(A)}(q^2, 0)}{M_B}. \end{aligned} \tag{2.8}$$

2. Direct emission of the virtual photon from valence quarks of the B-meson

Another contribution to the amplitude, $A^{(2)}_{\rm top}$, describes the process when the real photon is emitted from the penguin FCNC vertex, whereas the virtual photon is emitted from the valence quarks of the B-meson, see Fig. 1(c).

The amplitude $A^{(2)}_{\rm top}$ has the same Lorentz structure as the C_7 part of $A^{(1)}$ where now $k = q$, $k' = p - q$, $k'^2 = 0$, and $k^2 = q^2$. The amplitude thus involves the form factors $F_{TA,TV}(0, q^2)$, with $F_{TA}(0, q^2) = F_{TV}(0, q^2)$ (see details in Appendix A),

$$\begin{aligned} A^{(2)}_{\rm top} &= \langle \gamma(k'), l^+(p_1), l^-(p_2)|H^{b\to s\gamma}_{\rm eff}|\bar{B}_s(p)\rangle \\ &= \frac{G_F}{\sqrt{2}} V_{tb}V^*_{ts}\frac{\alpha_{\rm em}}{2\pi} e\varepsilon_\mu(k')\bar{l}(p_2)\gamma_\alpha l(-p_1) \\ &\quad \times [\epsilon_{\mu\alpha k' k}A^{(2)}_V(q^2) - i(g_{\mu\alpha}k'k - k'_\alpha k_\mu)A^{(2)}_A(q^2)], \\ k &= q, \quad k' = p - q, \end{aligned} \tag{2.9}$$

with

$$A^{(2)}_{V(A)}(q^2) = \frac{2m_b C_7(\mu)}{q^2} F_{TV(TA)}(0, q^2). \tag{2.10}$$

Obviously,

$$A^{(\bar{B}_s\to\gamma ll)}_{\rm top} = A^{(1)}_{\rm top} + A^{(2)}_{\rm top}. \tag{2.11}$$

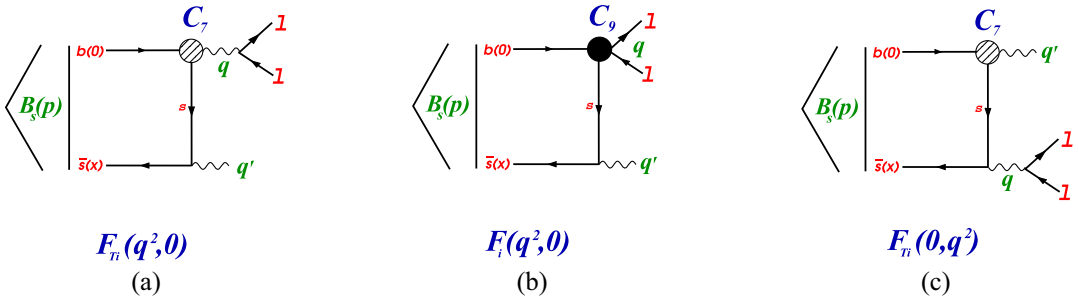

FIG. 1. Diagrams describing top-quark contributions to $\bar{B}_s \to \gamma l^+ l^-$ amplitude. Dashed circle denotes the O_7 operator, solid circle denotes the O_9 operator. Diagrams (a) and (b) describe the contribution $A^{(1)}$ where the real photon is emitted by spectator s-quark. Diagram (c) describes $A^{(2)}$ where the real photon is emitted from the penguin. We do not show $1/m_b$-suppressed diagrams where real or virtual photon is emitted by spectator b-quark, see [42] for details.

B. Charm-quark contribution

The charm-loop contribution to the $B_s \to \gamma l^+ l^-$ amplitude,

$$A^{(\bar{B}_s\to\gamma ll)}_{\text{charm}} = \langle\gamma(q')l^+(p_1)l^-(p_2)|H^{b\to s\bar{c}c}_{\text{eff}}|\bar{B}_s(p)\rangle, \quad q = p_1 + p_2, \tag{2.12}$$

is described by the diagrams of Fig. 2. $H^{b\to s\bar{c}c}_{\text{eff}}$ includes four-quark operators and may be written in the form

$$H^{b\to s\bar{c}c}_{\text{eff}} = H^{b\to s\bar{c}c[1\times1]}_{\text{eff}} + H^{b\to s\bar{c}c[8\times8]}_{\text{eff}}, \tag{2.13}$$

$$H^{b\to s\bar{c}c,[1\times1]}_{\text{eff}} = -\frac{G_F}{\sqrt{2}}V_{cb}V^*_{cs}\left(C_1+\frac{C_2}{3}\right)\bar{s}\gamma_\mu(1-\gamma_5) \times b\cdot\bar{c}\gamma_\mu(1-\gamma_5)c, \tag{2.14}$$

$$H^{b\to s\bar{c}c[8\times8]}_{\text{eff}} = -\frac{G_F}{\sqrt{2}}V_{cb}V^*_{cs}(2C_2)\bar{s}\gamma_\mu(1-\gamma_5) \times t^a b\cdot\bar{c}\gamma_\mu(1-\gamma_5)t^a c. \tag{2.15}$$

Let us introduce the amplitude of the transition into two virtual photons γ' and γ,

$$A^{(\bar{B}_s\to\gamma'\gamma)}_{\text{charm}} = \langle\gamma'(k')\gamma(k)|H^{b\to s\bar{c}c}_{\text{eff}}|\bar{B}_s(p)\rangle, \quad p = k' + k, \tag{2.16}$$

where the photon $\gamma'(k')$ is emitted by the c-quark, the photon $\gamma(k)$ is emitted from the s-quark and no symmetrization over photons is performed at this point (but is done later). The amplitude (2.16) may be written as [42]

$$\langle\gamma'(k')\gamma(k)|H^{b\to s\bar{c}c}_{\text{eff}}|\bar{B}_s(p)\rangle = -\varepsilon_\mu(k')\varepsilon_\alpha(k)H_{\mu\alpha}(k',k), \tag{2.17}$$

with

$$H_{\mu\alpha}(k',k) = i\int dx e^{ik'x}\langle 0|T\{eQ_c\bar{c}(x)\gamma_\mu c(x), eQ_s\bar{s}(0)\gamma_\alpha s(0)\}|\bar{B}_s(p)\rangle, \quad p = k + k'. \tag{2.18}$$

Here quark fields are understood as Heisenberg field operators with respect to all SM interactions. The matrix element (2.18) has the Lorentz structure dictated by conservation of charm-quark and strange-quark vector currents that requires $k^\alpha H_{\mu\alpha}(k',k)=0$ and $k'^\mu H_{\mu\alpha}(k',k)=0$ (notice the absence of any contact terms),

$$H_{\mu\alpha}(k',k) = -\frac{G_F}{\sqrt{2}}V_{cb}V^*_{cs}e^2\left[\epsilon_{\mu\alpha k'k}H_V - i(g_{\alpha\mu}kk' - k'_\alpha k_\mu)H_A - i\left(k'_\alpha - \frac{kk'}{k^2}k_\alpha\right)\left(k_\mu - \frac{kk'}{k'^2}k'_\mu\right)H_3\right], \tag{2.19}$$

with the invariant form factors H_i depending on two variables, $H_i(k'^2,k^2)$ (H_i include electric charges Q_s and Q_c). The singularities in the projectors at $k^2=0$ and $k'^2=0$ should not be the singularities of the amplitude $H_{\mu\alpha}(k',k)$, leading to the constraints,

$$H_3(k'^2=0,k^2) = H_3(k'^2,k^2=0) = 0. \tag{2.20}$$

As the result, H_3 does not contribute to the $B_s\to\gamma l^+l^-$ amplitude: to obtain the latter, $H_{\mu\alpha}$ should be multiplied by either $\epsilon^\alpha(k)\bar{l}\gamma_\mu l$ or $\epsilon^\mu(k')\bar{l}\gamma_\alpha l$. In each case, those terms in the H_3-part of $H_{\mu\alpha}$ containing k'_μ or k'_α vanish in the $B_s\to\gamma l^+l^-$ amplitude; the contribution of the 'regular' structure $k_\alpha k_\mu$ also vanishes because the form factor $H_3=0$ if $k^2=0$ or $k'^2=0$.

For the amplitude $A^{(\bar{B}_s\to\gamma ll)}_{\text{charm}}$ we obtain,

$$A^{(\bar{B}_s\to\gamma ll)}_{\text{charm}} = -\frac{eQ_l}{q^2}\{H_{\mu\alpha}(q,q')\bar{l}\gamma_\mu l\varepsilon_\alpha(q') + H_{\mu\alpha}(q',q)\varepsilon_\mu(q')\bar{l}\gamma_\alpha l\}, \quad Q_l=-1. \tag{2.21}$$

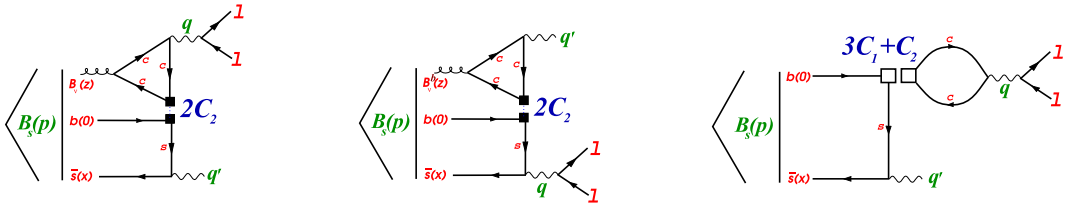

(a) (b) (c)

FIG. 2. The charm-loop contribution to the $B_s\to\gamma l^+l^-$ amplitude. (a) and (b) are nonfactorizable (NF) contributions induced by $H^{b\to s\bar{c}c[8\times8]}_{\text{eff}}$ (solid squares), (c) factorizable (F) contribution induced by $H^{b\to s\bar{c}c[1\times1]}_{\text{eff}}$ (empty squares); a similar factorizable contribution with the real photon emitted from the charm-quark loop vanishes and is not shown.

C. Summing top and charm contributions

Adding charm contributions to the top contributions and taking into account that $V_{tb}V_{ts}^* \simeq -V_{cb}V_{cs}^*$ leads to the following simple modifications [42]:

$$A_i^{(1)}(q^2) \to \frac{2C_7}{q^2} m_b F_{Ti}(q^2,0) + C_9 \frac{F_i(q^2,0)}{M_B} + 8\pi^2 \frac{H_i(q^2,0)}{q^2},$$
$$A_i^{(2)}(q^2) \to \frac{2C_7}{q^2} m_b F_{Ti}(0,q^2) + 8\pi^2 \frac{H_i(0,q^2)}{q^2}, \quad i = V, A. \tag{2.22}$$

The full amplitude is the sum of $A^{(1)}$ and $A^{(2)}$,

$$A_i(q^2) = \frac{2C_7}{q^2} m_b (F_{Ti}(q^2,0) + F_{Ti}(0,q^2)) + C_9 \frac{F_i(q^2,0)}{M_B} + 8\pi^2 \frac{H_i(q^2,0) + H_i(0,q^2)}{q^2}, \quad i = V, A. \tag{2.23}$$

The functions $H_i(k'^2, k^2)$ which contain factorizable and nonfactorizable charming loop contributions will be discussed in the next section.

III. CHARMING LOOP CONTRIBUTIONS TO $B_s \to \gamma^*\gamma^*$

In Eq. (2.18), quark fields are the Heisenberg operators in the SM, i.e., the corresponding S-matrix includes weak interactions of quarks. So we need to expand the S-matrix to the first order in weak interaction.

A. Factorizable contribution of the charming loop

Factorizable contributions of the charming loop emerge in

$$\mathcal{A}_{\text{charm,F}}^{(\bar{B}_s \to \gamma'\gamma)} = \langle \gamma'(k'), \gamma(k) | H_{\text{eff}}^{b\to s\bar{c}c[1\times 1]} | \bar{B}_s(p) \rangle, \tag{3.1}$$

when no gluons are exchanges between the charm-quark loop and the B-meson loop (whereas all gluon exchanges inside the loops are allowed). The corresponding $H_{\mu\alpha}^{\text{F}}(k', k)$ reads

$$H_{\mu\alpha}^{\text{F}}(k', k) = \frac{G_F}{\sqrt{2}} V_{cb}V_{cs}^* \frac{3C_1 + C_2}{3} eQ_c \Pi_{\mu\nu}^{cc}(k') \left(i \int dy e^{ik'y} \langle 0 | T\{\bar{s}\gamma_\nu(1-\gamma_5)b(y), eQ_s \bar{s}\gamma_\alpha s(0)\} | \bar{B}_s(p) \rangle \right), \tag{3.2}$$

where the expression in brackets is just the amplitude of (A2) and

$$\Pi_{\mu\nu}^{cc}(k') = i \int dx e^{ik'x} \langle 0 | T\{\bar{c}\gamma_\mu c(x), \bar{c}\gamma_\nu c(0)\} | 0 \rangle = (-g_{\mu\nu}k'^2 + k'_\mu k'_\nu) \Pi_{cc}(k'^2). \tag{3.3}$$

For the invariant function $\Pi_{cc}(s)$ we may write the spectral representation with one subtraction,

$$\Pi_{cc}(k'^2) = \Pi_{cc}(0) + \frac{k'^2}{\pi} \int \frac{\text{Im}\Pi_{cc}(s)}{s(s-k'^2)} ds. \tag{3.4}$$

At $k'^2 \ll 4m_c^2$, $\Pi_{cc}(k'^2)$ can be calculated in perturbative QCD. At leading order in α_s, one finds

$$\text{Im}\Pi_{cc}(s) = \frac{N_c}{12\pi} \frac{2m_c^2 + s}{s} \sqrt{1 - \frac{4m_c^2}{s}},$$
$$\Pi_{cc}(0) = \frac{9}{16\pi^2} \left\{ -\frac{8}{9} \ln\left(\frac{m_c}{m_b}\right) - \frac{4}{9} \right\}. \tag{3.5}$$

The factorizable contributions to the form factors $H_i(k'^2, k^2)$ are related to f, a_1, a_2 (see Appendix A) as follows

$$H_V^{\text{F}}(k'^2, k^2) = \frac{3C_1 + C_2}{3} Q_c k'^2 \Pi_{\bar{c}c}(k'^2) 2g(k'^2, k^2), \tag{3.6}$$

$$H_A^{\text{F}}(k'^2, k^2) = \frac{3C_1 + C_2}{3} Q_c k'^2 \Pi_{\bar{c}c}(k'^2) \frac{f(k'^2, k^2)}{kk'}, \tag{3.7}$$

$$H_3^{\text{F}}(k'^2, k^2) = \frac{3C_1 + C_2}{3} Q_c k'^2 \Pi_{\bar{c}c}(k'^2) \left\{ \frac{f}{kk'} + a_1 + a_2 \right\}. \tag{3.8}$$

Obviously, $H_{V,A,3}^{\text{F}}(k'^2 = 0, k^2) = 0$. Therefore, the factorizable $\bar{c}c$ contribution to the amplitude $A^{(2)}$ vanish; the $\bar{c}c$ contributions to $A^{(2)}$ comes exclusively from NF gluon exchanges. The factorizable contribution to $A^{(1)}$ takes the form [$H_3^{\text{F}}(k'^2, k^2 = 0) = 0$ because of the constraint (A4)]

$$H_i^{\text{F}}(q^2, 0) = \frac{3C_1 + C_2}{3} Q_c q^2 \Pi_{\bar{c}c}(q^2) \frac{F_i(q^2,0)}{M_B}, \quad i = A, V. \tag{3.9}$$

Since $3C_1 + C_2 < 0$ and for the $B_s \to \gamma$ transition $F_{V,A}(q^2, 0) > 0$ [42], we find that $H_{V,A}^{\text{F}}(q^2, 0) < 0$ at $q^2 > 0$.

Clearly, the factorizable $\bar{c}c$ contributions to $A^{(1)}$ can be described as a universal q^2-addition to the coefficient C_9,

$$C_9 \to C_9^{\rm eff}(q^2) = C_9 + \Delta^{\rm F} C_9(q^2),$$
$$\Delta^{\rm F} C_9(q^2) = 8\pi^2 Q_c \frac{3C_1 + C_2}{3} \Pi_{\bar{c}c}(q^2). \quad (3.10)$$

Taking into account that C_9, C_2, and $3C_1 + C_2$ have the same sign, and $\Pi_{\bar{c}c}(q^2) \geq 0$, we find that

$$\delta^{\rm F} C_9(q^2) \equiv \Delta^{\rm F} C_9(q^2)/C_9 > 0. \quad (3.11)$$

B. Nonfactorizable contribution of the charming loop

Nonfactorizable (NF) contributions of the charming loop emerge in

$$\mathcal{A}^{(\bar{B}_s \to \gamma'\gamma)}_{\rm charm,NF} = \langle \gamma'(k'), \gamma(k) | H_{\rm eff}^{b\to s\bar{c}c[8\times 8]} | \bar{B}_s(p) \rangle. \quad (3.12)$$

The corresponding $H^{\rm NF}_{\mu\alpha}$ has the form

$$H^{\rm NF}_{\mu\alpha}(k',k) = i^3 \frac{G_F}{\sqrt{2}} V_{cb} V^*_{cs} e^2 (2C_2) Q_c Q_s \int dz dx dy e^{ik'z} e^{iky}$$
$$\times \langle 0 | T\{\bar{c}\gamma_\mu c(z), \bar{c}(0) t^a \gamma_\beta (1-\gamma_5) c(0), \bar{c}(x) t^b \gamma_\nu c(x)\} | 0 \rangle$$
$$\times \langle 0 | T\{\bar{s}(y)\gamma_\alpha s(y), \bar{s}(0) t^a \gamma_\beta (1-\gamma_5) b(0) g_s B^b_\nu(x)\} | \bar{B}_s(p) \rangle. \quad (3.13)$$

This expression takes into account photon emission by the B-meson valence s-quark; a $1/m_b$-suppressed contribution related to photon emission by the valence b-quark will be omitted. We now outline the procedure of calculating $H^{\rm NF}_{\mu\alpha}$ and for all details refer to our recent paper [1]:

(1) The amplitude Eq. (3.13) includes the charm-quark loop contribution described by the $\langle VVA \rangle$ three-point function,

$$\Gamma^{\beta\nu\mu(ab)}_{cc}(\kappa, k') = \int dx' dz e^{ik'z + i\kappa x'} \langle 0 | T\{\bar{c}(z)\gamma^\mu c(z), \bar{c}(0)\gamma^\beta (1-\gamma_5) t^a c(0), \bar{c}(x')\gamma^\nu t^b c(x')\} | 0 \rangle$$
$$= \frac{1}{2} \delta^{ab} \Gamma^{\beta\nu\mu}_{cc}(\kappa, k'), \quad (3.14)$$

where k' is the momentum of the external virtual photon (vertex containing index μ) and κ is the gluon momentum (vertex containing index ν). Here t^c, $c = 1, \ldots, 8$ are $SU_c(3)$ generators normalized as $\mathrm{Tr}(t^a t^b) = \frac{1}{2}\delta^{ab}$.

The octet current $\bar{c}(0)\gamma^\beta(1-\gamma_5)t^a c(0)$ is a charm-quark part of the octet-octet weak Hamiltonian. Taking into account vector-current conservation, it is convenient to parametrize $\Gamma^{\beta\nu\mu}_{cc}(\kappa, k')$ as follows [43]:

$$\Gamma^{\beta\nu\mu}_{cc}(\kappa, k') = -i(\kappa^\beta + k'^\beta)\epsilon^{\nu\mu\kappa k'} F_0 - i(k'^2 \epsilon^{\beta\nu\mu\kappa} - k'^\mu \epsilon^{\beta\nu k'\kappa}) F_1 - i(\kappa^2 \epsilon^{\beta\mu\nu k'} - \kappa^\nu \epsilon^{\beta\mu\kappa k'}) F_2. \quad (3.15)$$

The form factors $F_{0,1,2}$ are functions of three independent invariant variables k'^2, κ^2, and $\kappa k'$. We use a convenient representation of the one-loop form factors in the form [1],

$$F_i(\kappa^2, \kappa k', k'^2) = \frac{1}{\pi^2} \int_0^1 d\xi \int_0^{1-\xi} d\eta \frac{\Delta_i(\xi,\eta)}{m_c^2 - 2\xi\eta\kappa k' - \xi(1-\xi)k'^2 - \eta(1-\eta)\kappa^2}, \quad i = 0,1,2,$$
$$\Delta_0 = -\xi\eta, \qquad \Delta_1 = \xi(1-\eta-\xi), \qquad \Delta_2 = \eta(1-\eta-\xi). \quad (3.16)$$

As shown in Sec. III of [1], the operator describing the contribution of the charm-quark loop may be written in the form containing only $G^a_{\nu\alpha}$,

$$\int d\kappa e^{-i\kappa x} \Gamma^{\beta\nu\mu(ab)}_{cc}(\kappa, k') B^b_\nu(x) dx = \frac{1}{4} \int d\kappa e^{-i\kappa x} \bar{\Gamma}^{\beta\nu\mu\xi}_{cc}(\kappa, k') G^a_{\nu\xi}(x) dx, \quad (3.17)$$

with

$$\bar{\Gamma}^{\beta\nu\mu\xi}_{cc}(\kappa, k') = (\kappa^\beta + k'^\beta)\epsilon^{\nu\mu\xi k'} F_0 + (k'^\mu \epsilon^{\beta\nu\xi k'} + k'^2 \epsilon^{\beta\nu\mu\xi}) F_1 + (\kappa^\beta \epsilon^{\xi\nu\mu k'} + \kappa^\mu \epsilon^{\xi\beta\nu k'} - \kappa k' \epsilon^{\xi\beta\nu\mu}) F_2. \quad (3.18)$$

(2) Making use of this result for the charm-quark $\langle VVA\rangle$ triangle, we have

$$H^{\rm NF}_{\mu\alpha} = -\frac{G_F}{\sqrt{2}} V_{cb}V^*_{cs} e^2 (2C_2) Q_s Q_c \tilde{H}^{\rm NF}_{\mu\alpha}(k',k), \tag{3.19}$$

$$\tilde{H}^{\rm NF}_{\mu\alpha}(k',k) = \frac{1}{4(2\pi)^8}\int d\tilde{k}dy e^{-i(\tilde{k}-k)y} dx d\kappa e^{-i\kappa x} \bar{\Gamma}^{\beta\nu\mu\xi}_{cc}(\kappa,k')\langle 0|\bar{s}(y)\gamma^\eta \frac{\tilde{k}+m_s}{m_s^2-\tilde{k}^2}\gamma^\mu(1-\gamma^5)t^b G^b_{\nu\xi}(x) b(0)|\bar{B}_s(p)\rangle. \tag{3.20}$$

For $k'^2=0$ or $k^2=0$, $\tilde{H}^{\rm NF}_{\mu\alpha}$ contains two form factors,

$$\tilde{H}^{\rm NF}_{\mu\alpha}(k',k) = \tilde{H}^{\rm NF}_V \epsilon_{\mu\alpha k' k} - i\tilde{H}^{\rm NF}_A (g_{\rho\eta} k'k - k_\mu k'_\alpha), \tag{3.21}$$

such that

$$H^{\rm NF}_i(k'^2,k^2) = 2C_2 Q_s Q_c \tilde{H}^{\rm NF}_i(k'^2,k^2). \tag{3.22}$$

(3) The B-meson structure contributes to $H^{\rm NF}_{\mu\alpha}$ via the full set of 3BS,

$$\langle 0|\bar{s}(y)\Gamma_i t^a b(0) G^a_{\nu\alpha}(x)|\bar{B}_s(p)\rangle, \tag{3.23}$$

with Γ_i the appropriate combinations of γ-matrices. This quantity is not gauge invariant, since it contains field operators at different locations. To make it gauge-invariant, one needs to insert Wilson lines between the field operators. To simplify the full consideration, it is convenient to work in a fixed-point gauge, where the Wilson lines reduce to unity factors.

When the coordinates x and y are independent variables, the 3BS has the following decomposition [1]:

$$\begin{aligned}\langle 0|\bar{s}(y)G_{\nu\xi}(x)\Gamma b(0)|\bar{B}_s(p)\rangle =& \frac{f_B M_B^3}{4}\int D(\omega,\lambda) e^{-i\lambda yp - i\omega xp}{\rm Tr}\Big\{\gamma_5\Gamma(1+\not{v})\\ &\times\Big[(p_\nu\gamma_\xi - p_\xi\gamma_\nu)\frac{1}{M_B}[\Psi_A-\Psi_V] - i\sigma_{\nu_\xi}\Psi_V - \frac{(x_\nu p_\xi - x_\xi p_\nu)}{xp}\Big(X_A^{(x)} + \frac{\not{x}}{xp}M_B W^{(x)}\Big)\\ &+\frac{(x_\nu\gamma_\xi - x_\xi\gamma_\nu)}{xp}M_B\Big(Y_A^{(x)} + W^{(x)} + \frac{\not{x}}{xp}M_B Z^{(x)}\Big) - \frac{(y_\nu p_\xi - y_\xi p_\nu)}{yp}\Big(X_A^{(y)} + \frac{\not{y}}{yp}M_B W^{(y)}\Big)\\ &+\frac{(y_\nu\gamma_\xi - y_\xi\gamma_\nu)}{yp}M_B\Big(Y_A^{(y)} + W^{(y)} + \frac{\not{y}}{yp}M_B Z^{(y)}\Big) - i\epsilon_{\nu\xi\mu\beta}\frac{x^\mu p^\beta}{xp}\gamma^5\tilde{X}_A^{(x)}\\ &+i\epsilon_{\nu\xi\mu\beta}\frac{x^\mu\gamma^\beta}{xp}\gamma^5 M_B\tilde{Y}_A^{(x)} - i\epsilon_{\nu\xi\mu\beta}\frac{x^\mu p^\beta}{xp}\gamma^5\tilde{X}_A^{(y)} + i\epsilon_{\nu\xi\mu\beta}\frac{x^\mu\gamma^\beta}{xp}\gamma^5 M_B\tilde{Y}_A^{(y)}\Big]\Big\},\end{aligned} \tag{3.24}$$

where

$$D(\omega,\lambda) = d\omega d\lambda\theta(\omega)\theta(\lambda)\theta(1-\omega-\lambda) \tag{3.25}$$

takes into account rigorous constraints on the variables ω and λ. All invariant amplitudes $\Phi = \Psi_A, \Psi_V, \ldots$ are functions of five variables, $\Phi(\omega,\lambda,x^2,y^2,xy)$, for which we may write Taylor expansion in x^2, y^2, xy. Here we limit our analysis to zero-order terms in this expansion. The corresponding zero-order terms in Φ's are functions of dimensionless arguments λ and ω and are referred to as the Lorentz 3DAs.

The normalization conditions for Ψ_A and Ψ_V have the form [24],

$$\begin{aligned}\int D(\omega,\lambda)\Psi_A(\omega,\lambda) &= \frac{\lambda_E^2}{3M_B^2},\\ \int D(\omega,\lambda)\Psi_V(\omega,\lambda) &= \frac{\lambda_H^2}{3M_B^2}.\end{aligned} \tag{3.26}$$

A number of Lorentz structures in (3.24) contain singularities at $xp=0$ and $yp=0$. Since 3BS (3.24) is a continuous regular function at the point $x^2=0$, $y^2=0$, $xp=0$, $yp=0$, the absence of singularities at $xp\to 0$ and $yp\to 0$ leads to a number of constraints on the corresponding 3DAs [31]; namely, the primitives of these 3DAs should vanish at the boundaries of the 3DA support regions. The appropriate modifications of 3DAs at the upper

endpoint region of ω and λ have been developed in [1]. Here we follow the approach of [1] and refer to that publication for details.

(4) Making use of Eq. (3.24) (i) reduces the matrix element in Eq. (3.20) to trace calculation and (ii) reduces the integrations over x and y to $\delta(\kappa+\omega p)\delta(\tilde{k}-k+\lambda p)$ (see details in [1]). Using these δ-functions to integrate over κ and k, the form factors H_i, $i=A,V$ are obtained as integrals of the form

$$\tilde{H}_i^{\rm NF}(k'^2,k^2)=\int_0^{2\omega_0}d\omega\int_0^{2\omega_0-\omega}d\lambda\int_0^1 d\xi \times\int_0^{1-\xi}d\eta\tilde{h}_i^{\rm NF}(\omega,\lambda,\xi,\eta|k'^2,k^2). \quad (3.27)$$

Here $\tilde{h}_i$ are linear combinations of the 3DAs entering Eq. (3.24) and their primitives, and include the form factors $F_{0,1,2}$ describing the charming $\langle VVA\rangle$ triangle and the s-quark propagator. As an illustration, we present the leading part of the ψ_A and ψ_V contribution to $\tilde{h}_V^{\rm NF}(k'^2,k^2)$ [neglecting in the numerator all powers of $\lambda=O(\Lambda_{\rm QCD}/m_b)$ and $\omega=O(\Lambda_{\rm QCD}/m_b)$]

$$\tilde{h}_V(\omega,\lambda,\xi,\eta|k'^2,k^2) =-\frac{\frac{1}{2}f_BM_B^4}{m_s^2+\lambda(1-\lambda)M_B^2-(1-\lambda)k^2-\lambda k'^2} \times\{(\Psi_A+\Psi_V)[(M_B^2+k'^2-k^2)F_0-2k'^2F_1] -2\Psi_Ak'^2[F_0-3F_1]\}. \quad (3.28)$$

The form factors $F_{0,1,2}$ given by Eq. (3.16) depend on ξ and η and should be evaluated for $\kappa=-\omega p$. Notice that $F_0<0$ and thus $\tilde{H}_V(k'^2,k^2)>0$; the form factor $\tilde{H}_A(k'^2,k^2)$ turns out numerically close to $\tilde{H}_V(k'^2,k^2)$.[2]

IV. RESULTS FOR THE $B_s\to\gamma l^+l^-$ NF CHARMING-LOOP FORM FACTOR

Our further calculation directly follows the approach of [1] with the difference that now both photons are virtual.

A. Model for 3DAs

Following [1], we make use of the set of 3DAs of local-duality (LD) model of [24,44] and perform the appropriate modifications of the 3DAs $X_A^{(x)},X_A^{(y)},\ldots$. All necessary details including the explicit expressions of the 3DAs are given in Sec. IV of [1] and will not be repeated here. As a reference, we present just the Lorentz 3DAs Ψ_A and Ψ_V of the LD model [24],

$$\Psi_A(\omega,\lambda)=(\phi_3+\phi_4)/2,\qquad \Psi_V(\omega,\lambda)=(-\phi_3+\phi_4)/2 \quad (4.1)$$

with

$$\phi_3=\frac{105(\lambda_E^2-\lambda_H^2)}{32\omega_0^7M_B^2}\lambda\omega^2(2\omega_0-\omega-\lambda)^2\theta(2\omega_0-\omega-\lambda), \quad (4.2)$$

$$\phi_4=\frac{35(\lambda_E^2+\lambda_H^2)}{32\omega_0^7M_B^2}\omega^2(2\omega_0-\omega-\lambda)^3\theta(2\omega_0-\omega-\lambda). \quad (4.3)$$

Dimensionless parameter ω_0 is related to λ_B, the inverse moment of the B-meson LC distribution amplitude, as

$$\omega_0=\frac{5}{2}\frac{\lambda_B}{M_B}. \quad (4.4)$$

For this model, the integration limits take the following form ($2\omega_0<1$):

$$\int D(\omega,\lambda)\theta(2\omega_0-\omega-\lambda)(\ldots)=\int_0^{2\omega_0}d\omega\int_0^{2\omega_0-\omega}d\lambda(\ldots). \quad (4.5)$$

The form factors $H_{A,V}(k'^2,k^2)$ have explicit linear dependence on $\lambda_{E,H}^2$, so we write

$$H_i^{\rm NF}(k'^2,k^2)=2C_2Q_sQ_c[R_{iE}(k'^2,k^2)\lambda_E^2+R_{iH}(k'^2,k^2)\lambda_H^2], \quad i=A,V. \quad (4.6)$$

QCD sum rules suggest an approximate relation [24],

$$\lambda_H^2\simeq 2\lambda_E^2. \quad (4.7)$$

Then, the appropriate combinations of the form factors which describe NF charm contributions have the form

$$R_i(k'^2,k^2)=R_{iE}(k'^2,k^2)+2R_{iH}(k^2,k^2),\qquad H_i(k'^2,k^2)=2C_2Q_sQ_c\lambda_E^2R_i(k'^2,k^2),\qquad i=A,V. \quad (4.8)$$

Combining (4.7) with QCD equations of motion, 3BS model used in our analysis leads to approximate relations

$$\lambda_H^2\simeq 1.2\lambda_{B_s}^2,\qquad \lambda_E^2\simeq 0.6\lambda_{B_s}^2. \quad (4.9)$$

[2]Analytic expressions for $\tilde{h}_i$, $i=A,V,3$ as a *Mathematica* file may be obtained from the authors upon request.

This leads to an explicit linear dependence of H_i on $\lambda_{B_s}^2$. It should be noticed however that the form factors have also a complicated implicit dependence on λ_{B_s} through a λ_{B_s}-dependent shape of the three-particle distribution amplitudes of B_s. We present below our results for the benchmark point [1],

$$\lambda_{B_s}(1\ \text{GeV}) = 0.45\ \text{GeV}. \tag{4.10}$$

For a discussion of the existing estimates of λ_{B_s} and $\lambda_{E,H}^2$ including their dependence on the scale, we refer to [45–54]. A remark may be useful before we go to the results for the form factors; the parameters $\lambda_{E,H}^2$ as well as the parameter λ_{B_s} depend on the scale. We do not discuss this dependence and perform numerical calculations just assuming that the form factors are represented in terms of these parameters at a fixed scale 1 GeV as given in (4.9) and (4.10). The parameter λ_{B_s} is presently not known with good accuracy (see [53]) and at the same time one observes a sizeable sensitivity of the form factors $H_i^{\rm NF}$ to its value [see Fig. 7 in [1] for the form factor $H_i^{\rm NF}(0,0)$]. In this situation, studying the scale dependence of the form factors $H_i^{\rm NF}(k'^2, k^2)$ induced by the scale dependence of λ_{B_s} would not be useful.

B. Results for the form factors $H_i^{\rm NF}(k'^2,k^2)$

The analytic expressions (3.27) are based on finite-order QCD diagrams and thus cannot be trusted near quark thresholds. For instance, the calculated form factors exhibit steep rise at negative $k^2 \to 0$ which is unphysical, as the nearest hadron pole lies at $k^2 = M_\phi^2$ and the two-meson threshold lies at $k^2 = 4M_K^2$.

We therefore pursue the strategy previously applied in [1,55] to the form factors of one variable, and extend it to the case of $R_i(k'^2, k^2)$ depending on two variables: We first calculate the form factors $R_i(k'^2, k^2)$ using the analytic expressions (3.27) in the rectangular region relatively far from quark thresholds in QCD diagrams,

$$0 < k'^2(\text{GeV}^2) < 4, \qquad -5 < k^2(\text{GeV}^2) < -0.6. \tag{4.11}$$

We then interpolate the results obtained in this region as function of two variables k'^2 and k^2 by a formula (C1) which takes into account the correct location of the hadron poles at $k'^2 = M_{J/\psi}^2$ and $k^2 = M_\phi^2$ and contains a number of fit parameters allowing us to fit $R_i(k'^2, k^2)$ in the rectangular region (4.11) with an accuracy of not worse than 2%. The fit formula and its parameters obtained by this procedure are given in Appendix C. Finally, since our interpolating formula takes into account correct location of the lowest meson poles in the k'^2 and k^2 channels, we find it

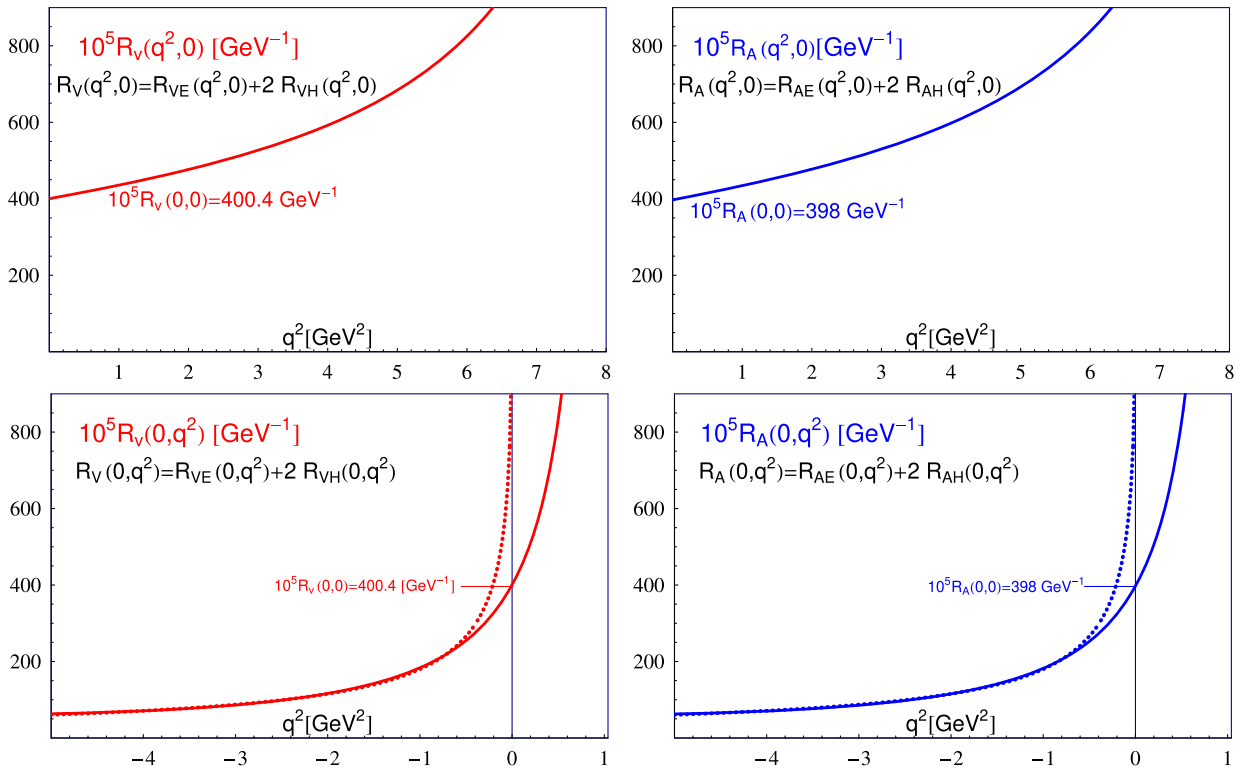

FIG. 3. Solid lines are the fits. For $R(0, q^2)$, dashed lines present the results of direct calculations.

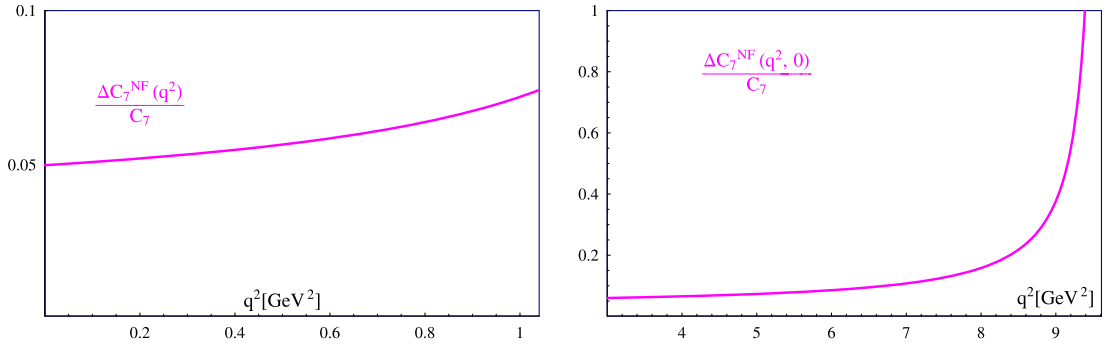

FIG. 4. (a) The relative NF correction $\delta_V^{\rm NF}C_7(q^2)$ given by Eq. (4.13). (b) $\delta^{\rm NF}C_7(q^2,0)$ given by Eq. (4.13) which dominates in $\delta_V^{\rm NF}C_7(q^2)$ for $q^2 > 3$ GeV^2.

eligible to use this formula to extrapolate the form factors to the region of timelike momenta $k'^2 \le M_{J/\psi}^2$ and $k^2 \le 4M_K^2$.

Figure 3 shows our numerical predictions for the NF form factors corresponding to the central values of all parameters, for the discussion we refer to [1]. As reported in [1], the accuracy of the predictions for the form factors depend sizebly on λ_{B_s}. However, for a given value of λ_{B_s}, the form factors $H_i(k'^2, k^2)$ may be calculated with an accuracy around 10%.

C. NF charm vs top

The effect of factorizable charming loops may be conveniently described as a process-independent but q^2-dependent correction to the Wilson coefficient C_9, Eq. (3.10), with $\delta^{\rm F}C_9(q^2) > 0$.

One may in principle describe also NF charming-loop contribution as a correction to C_9; in this case, however, the correction explodes at small q^2. So it is more natural to describe the effect of NF charm in $B_s \to \gamma ll$ as additions to the Wilson coefficient C_7 related to different $A_i(q^2)$ ($i = A$, V) in Eq. (2.23),

$$A_V(q^2):\ C_7 \to C_7 + \Delta_V^{\rm NF}C_7(q^2),$$
$$A_A(q^2):\ C_7 \to C_7 + \Delta_A^{\rm NF}C_7(q^2), \qquad (4.12)$$

with the relative correction

$$\delta_i^{\rm NF}C_7(q^2) = \frac{\Delta_i^{\rm NF}C_7(q^2)}{C_7} = 8\pi^2 Q_s Q_c \frac{C_2}{C_7}\frac{1}{m_b}\frac{\tilde H_i^{\rm NF}(q^2,0) + \tilde H_i^{\rm NF}(0,q^2)}{F_{Ti}(q^2,0) + F_{Ti}(0,q^2)}, \quad i = A, V. \qquad (4.13)$$

The form factors $F_{Ti}(k'^2, k^2)$ have been evaluated using the 2DAs $\phi_\pm$ belonging to the same set of the distribution amplitudes as the 3DAs (4.2) and (4.3), see details in [1]. Convenient parametrizations for the form factors $F_{Ti}(k'^2, k^2)$ in a broad range of their momenta are given in Appendix D.

The Wilson coefficients C_2 and C_7 have opposite signs, $\tilde H_i^{\rm NF}(q^2,0)$ and $\tilde H_i^{\rm NF}(0,q^2)$ as well as $F_{Ti}(q^2,0)$ and $F_{Ti}(0,q^2)$ are positive [42]. So, the relative correction $\delta_i^{\rm NF}C_7$ is found to be positive

$$\delta_i^{\rm NF}C_7(q^2) > 0. \qquad (4.14)$$

Numerically, $\delta_A^{\rm NF}C_7(q^2) \simeq \delta_V^{\rm NF}C_7(q^2)$. The form factors $H_i(q^2,0)$ are predicted in the region $q^2 < M_{J/\psi}^2$, whereas $H_i(0,q^2)$ is predicted in the region $q^2 < 4M_K^2$ [recall that at $q^2 > 4M_K^2$, $H_i(0,q^2)$ have imaginary part]. In principle, one can model $H_i(0,q^2)$ for $q^2 > 4M_K^2$, but this interesting problem is beyond the scope of this paper. So, Fig. 4(a) presents $\delta_i^{\rm NF}C_7(q^2)$ in the range $0 < q^2 < 4M_K^2$, where our predictions are less model dependent. On the other hand, as the analysis of [42] has shown, for $q^2 \ge 3$ GeV^2 (i.e., far above M_ϕ^2), the contribution of the amplitude $H_i^{\rm NF}(0,q^2)$ turns out to be much suppressed compared to $H_i^{\rm NF}(q^2,0)$. The same occurs for the form factor F_{Ti}; in this range of q^2, $F_{Ti}(q^2,0) \gg F_{Ti}(0,q^2)$. Therefore the contribution of $H_i^{\rm NF}(0,q^2)$ in the numerator and the contribution of $F_{Ti}(0,q^2)$ in the denominator of (4.13) may be neglected [one however might need to be careful as both $H_i^{\rm NF}(0,q^2)$ and $H_i^{\rm NF}(0,q^2)$ have imaginary parts at $q^2 > 4M_K^2$]. Then the main contribution to $\delta^{\rm NF}C_7(q^2)/C_7$ in this range of q^2 is expected to come from the ratio $\frac{H_i^{\rm NF}(q^2,0)}{F_{Ti}(q^2,0)}$. This contribution is denoted as

$$\delta_i^{\rm NF}C_7(q^2,0) = \Delta_i^{\rm NF}C_7(q^2,0)/C_7, \qquad (4.15)$$

and is shown in Fig. 4(b) for $i = V$. Closing this section, we would like to emphasize that factorizable and nonfactorizable contributions of the charming loops, $H_i^{\rm F}$ and $H_i^{\rm NF}$, have opposite signs.

V. DISCUSSION AND CONCLUSIONS

This paper extended the theoretical approach to NF charming loops in FCNC B_s decays recently formulated in [1] and for the first time reports the results for NF charm in $B_s \to \gamma ll$ decays:

(i) We derived analytical expressions for the form factors $H_i^{\rm NF}(k'^2, k^2)$, $i = A, V$, describing NF contribution of charming loops to the amplitude of the B_s meson transition into two virtual photons (the first argument, k'^2 corresponds to the momentum emitted from the charming loop, whereas the second argument, k^2, corresponds to the momentum emitted by the valence s-quark of the B_s-meson). These expressions may be written in the form

$$H_i^{\rm NF}(k'^2, k^2) = 2C_2 Q_s Q_c [\lambda_E^2 R_{iE}(k'^2, k^2) + \lambda_H^2 R_{iH}(k'^2, k^2)] \quad i = A, V, 3. \tag{5.1}$$

Since an approximate relation $\lambda_H^2 \simeq 2\lambda_E^2$ is expected, the linear combination

$$R_i(k'^2, k^2) = 2R_{iH}(k'^2, k^2) + R_{iE}(k'^2, k^2) \tag{5.2}$$

is appropriate for the description of NF charming loops in B_s decays such that

$$H_i^{\rm NF}(k'^2, k^2) = 2C_2 Q_s Q_c \lambda_E^2 R_i(k'^2, k^2). \tag{5.3}$$

We emphasize that according to our analysis, $R_i(k'^2, k^2) > 0$ in the region $k'^2 < M_{J/\psi}^2$ and $k^2 < M_\phi^2$ and thus $H_i^{\rm NF}(k'^2, k^2)$ is positive in this region. Recall that the factorizable contribution $H_i^{\rm F}(k'^2, k^2)$ is negative.

(ii) The analytic expressions allow one to calculate the form factors $R_i(k'^2, k^2)$ in a broad range $k'^2 < 4m_c^2$ and $k^2 < 0$. However, calculations based on finite-order QCD diagrams are not expected to provide good description of the physical hadron amplitudes near quark thresholds (for instance, the calculated form factors exhibit steep rise at $k^2 \to 0$ which is unphysical, as the nearest meson pole lies at $k^2 = M_\phi^2$ and the two-meson threshold lies at $k^2 = 4M_K^2$). So we pursue the following strategy. We make use of the results of our calculation in the rectangular region $0 < k'^2({\rm GeV}^2) < 4$ and $-5 < k^2({\rm GeV}^2) < -0.6$ (i.e., sufficiently far from quark thresholds) and interpolate them by a simple analytic formula depending on k'^2 and k^2, which takes into account the presence of the poles at $k'^2 = M_{J/\psi}^2$ and $k^2 = M_\phi^2$. Numerical parameters in this formula are obtained by the fit to the results of our calculations and interpolate them with a 2% accuracy in the rectangular region mentioned above. The corresponding easy-to-use fit formulas for $R_i(k'^2, k^2)$ are presented in Appendix C.

(iii) Since the interpolating formulas exhibit the correct location of the lowest hadron singularities, i.e., poles at $k'^2 = M_{J/\psi}^2$ and at $k^2 = M_\phi^2$, our fit formulas are expected to provide reliable theoretical predictions for the form factors in a broader range $0 < k'^2 < M_{J/\psi}^2$ and $-5\ {\rm GeV}^2 < k'^2 < M_\phi^2$. Figure 3 shows $R_i(0, q^2)$ and $R_i(q^2, 0)$ related to $B_s \to \gamma ll$ decays.

(iv) The contribution of factorizable charm in $B_s \to \gamma ll$ decay may be treated as the q^2-dependent correction to the Wilson coefficient C_9, such that $\Delta^{\rm F} C_9(q^2)/C_9 > 0$ at $q^2 < M_{J/\psi}^2$. At the same time, the contribution of nonfactorizable charm in $B_s \to \gamma ll$ decay may be conveniently treated as the q^2-correction to the Wilson coefficient C_7, such that $\Delta^{\rm NF} C_7(q^2)/C_7 > 0$ at $q^2 < 4M_K^2$ (at higher values of q^2 the physical NF charming loop has imaginary part). Figure 4 presents our prediction for these quantities[3];

(v) Our numerical results for the form factors $H_i^{\rm NF}(k'^2, k^2)$ depend sizeably on the precise value of the parameter λ_{B_s}. In this respect we see the same picture as for the $B_s \to \gamma\gamma$ decay, see Fig. 7 in [1]. And, similar to the form factors for $B_s \to \gamma\gamma$ decay, for a fixed value of λ_{B_s}, $H_i^{\rm NF}(k'^2, k^2)$ may be calculated with about 10% accuracy.

It might be useful to recall that the $B_s \to \gamma ll$ decay amplitude receives contributions from the weak-annihilation type diagrams [56–59]. The weak-annihilation mechanism differs very much from the mechanism discussed in this paper and is therefore beyond the scope of our interest here. However, weak-annihilation diagrams should be taken into account in a complete analysis of $B_s \to \gamma ll$ decays.

ACKNOWLEDGMENTS

We are pleased to express our gratitude to Yu-Ming Wang for his illuminating remarks and comments and to Otto Nachtmann, Hagop Sazdjian, and Silvano Simula for valuable discussions. D. M. gratefully acknowledges participation at the Erwin Schrödinger Institute (ESI) thematic program "Quantum Field Theory at the Frontiers of the Strong Interaction" which promoted a deeper understanding of the problems discussed in this paper. The research was carried out within the framework of the program "Particle Physics and Cosmology" of the National Center for Physics and Mathematics.

[3]One may in principle interpret NF charm correction as $\Delta^{\rm NF} C_9$ instead of interpreting it as $\Delta^{\rm NF} C_7$ correction as we do here. In this case, $\Delta^{\rm NF} C_9(q^2)/C_9$ comes out negative and explodes at small q^2, so we do not find this possibility to be attractive.

APPENDIX A: CONSTRAINTS ON THE TRANSITION FORM FACTORS

We present here a discussion of the constraints imposed by the electromagnetic gauge invariance on the $\langle\gamma^*|\bar{q}O_i b|\bar{B}_q(p)\rangle$ transition amplitudes induced by the vector, axial-vector, tensor, and pseudotensor weak currents. This discussion extends the discussion of [41] and includes also the case when the real photon is emitted from the FCNC $b\to q$ vertex. The corresponding form factors are functions of two variables, k'^2 and k^2, where k' is the momentum of the weak $b\to q$ current, and k is the momentum of the electromagnetic current, $p=k+k'$. Gauge invariance provides constraints on some of the form factors describing the transition of B_q to the real photon emitted directly from the quark line, i.e., for the form factors at $k^2=0$.

These form factors fully determine the amplitudes of the FCNC B-decays into leptons in the final state. For instance, the four-lepton decay of the B meson requires the form factors $f_i(k'^2,k'^2)$ for $0<k^2,k'^2<M_B^2$. For the case of the $B\to\gamma l^+l^-$ transition one needs the form factors $f_i(k'^2=q^2,k'^2=0)$ and $f_i(k'^2=0,k'^2=q^2)$, where q is the momentum of the l^+l^- pair.

1. Form factors of the vector weak current

In case of the vector FCNC current, the gauge-invariant amplitude contains one form factor $g(k'^2,k^2)$,

$$T_{\alpha,\mu}=i\int dx e^{ikx}\langle 0|T\{j^{\rm em}_\alpha(x),\bar{q}\gamma_\mu b(0)\}|\bar{B}_q(p)\rangle = e\epsilon_{\mu\alpha k'k}2g(k'^2,k^2). \tag{A1}$$

The amplitude is automatically transverse and is free of the kinematic singularities so no constraints on $g(k'^2,k^2)$ emerge.

2. Form factors of the axial-vector weak current

For the axial-vector current, the corresponding amplitude has three independent gauge-invariant structures and three form factors, and in addition has the contact term which is fully determined by the conservation of the electromagnetic current, $\partial^\mu j^{\rm em}_\mu=0$,

$$\begin{aligned}T^5_{\alpha,\mu}&=i\int dx e^{ikx}\langle 0|T\{j^{\rm em}_\alpha(x),\bar{q}\gamma_\mu\gamma_5 b(0)\}|\bar{B}_q(p)\rangle\\&=ie\left(g_{\mu\alpha}-\frac{k_\alpha k_\mu}{k^2}\right)f(k'^2,k^2)\\&\quad+ie\left(k'_\alpha-\frac{kk'}{k^2}k_\alpha\right)[p_\mu a_1(k'^2,k^2)+k_\mu a_2(k'^2,k^2)]\\&\quad+iQ_{B_q}ef_{B_q}\frac{k_\alpha p_\mu}{k^2}.\end{aligned} \tag{A2}$$

Here $Q_{\bar{B}_q}=Q_b-Q_q$ is the electric charge of the $\bar{B}_q$ meson and $f_{\bar{B}_q}>0$ is defined according to

$$\langle 0|\bar{q}\gamma_\mu\gamma_5 b|\bar{B}_q(p)\rangle=if_{\bar{B}_q}p_\mu. \tag{A3}$$

The kinematical singularity in the projectors at $k^2=0$ should not be the singularity of the amplitude, and therefore gauge invariance yields the following relation between the form factors at $k^2=0$:

$$[f+(k'k)a_2]_{k^2=0}=0,\qquad a_1(k'^2,k^2=0)=Q_{\bar{B}_q}f_{\bar{B}_q}. \tag{A4}$$

For the neutral $\bar{B}_{d,s}$ mesons, the contact term is absent and therefore the form factor a_1 should vanish at $k^2=0$, $a_1(k'^2,k^2=0)=0$. This relation is fulfilled automatically, as the two contributions, corresponding to the photon emission from the valence b-quark and from the valence s, d-quark cancel each other at $k^2=0$.

The amplitude of the transition to the real photon is described by a single form factor,

$$\langle\gamma(k)|\bar{q}\gamma_\mu\gamma_5 b|\bar{B}_q(p)\rangle = -ie\varepsilon^\alpha(k)(g_{\mu\alpha}k'k-k'_\alpha k_\mu)a_2(k'^2,k^2=0). \tag{A5}$$

3. Form factors of the tensor weak current

The transition amplitudes induced by the tensor weak current can be decomposed in the Lorentz structures transverse with respect to k_α,

$$\begin{aligned}T_{\alpha,\mu\nu}&=i\int dx e^{ikx}\langle 0|\{Tj^{\rm em}_\alpha(x),\bar{q}\sigma_{\mu\nu}b(0)\}|\bar{B}_q(p)\rangle\\&=ie\left(\epsilon_{\mu\nu\alpha p}-\frac{k_\alpha}{k^2}\epsilon_{\mu\nu kp}\right)g_1(k'^2,k^2)+ie\epsilon_{\mu\nu\alpha k}g_2(k'^2,k^2)\\&\quad+ie\left(p_\alpha-\frac{pk}{k^2}k_\alpha\right)\epsilon_{\mu\nu k'k}g_0(k'^2,k^2).\end{aligned} \tag{A6}$$

The contact terms are absent in this amplitude as well as in the amplitude of the pseudotensor current. The kinematic singularity of the projectors at $k^2=0$ should not be the singularity of the amplitude, therefore

$$[g_1-(kp)g_0]_{k^2=0}=0. \tag{A7}$$

Multiplying (A6) by k'_ν, we obtain the penguin transition amplitude,

$$i\int dx e^{ikx}\langle 0|\{Tj^{\rm em}_\alpha(x),\bar{q}\sigma_{\mu\nu}k'^\nu b(0)\}|\bar{B}_q(p)\rangle = ie\epsilon_{\mu\alpha kp}(g_1+g_2). \tag{A8}$$

Notice that the penguin amplitude contains only one combination of the form factors. Nevertheless, the

requirement of the regularity of the amplitude (A6) yields the constraint (A7).

4. Form factors of the pseudotensor weak current

The transition amplitude of the pseudotensor weak current is given in terms of the same form factors as the amplitude (A6), and, similar to (A6), contains no contact terms,

$$\begin{aligned} T^5_{\alpha,\mu\nu} &= i\int dx e^{ikx}\langle 0|\{Tj^{\rm em}_\alpha(x),\bar q\sigma_{\mu\nu}\gamma_5 b(0)\}|\bar B_q(p)\rangle \\ &= \left[\left(g_{\alpha\nu}-\frac{k_\alpha k_\nu}{k^2}\right)p_\mu-\left(g_{\alpha\mu}-\frac{k_\alpha k_\mu}{k^2}\right)p_\nu\right]eg_1 \\ &\quad+(g_{\alpha\nu}k_\mu-g_{\alpha\mu}k_\nu)eg_2 \\ &\quad+\left(p_\alpha-\frac{k\cdot p}{k^2}k_\alpha\right)(k_\mu p_\nu-p_\nu k_\mu)eg_0. \end{aligned} \tag{A9}$$

The kinematical singularity in the projectors at $k^2=0$ should cancel in the amplitude, again leading to the constraint in Eq. (A7).

For the penguin pseudotensor amplitude we then obtain,

$$\begin{aligned} &i\int dx e^{ikx}\langle 0|\{Tj^{\rm em}_\alpha(x),\bar q\sigma_{\mu\nu}\gamma_5 k'^\nu b(0)\}|\bar B_q(p)\rangle \\ &=e(k'_\alpha k_\mu-g_{\alpha\mu}kk')\left\{g_1+g_2+\frac{k'^2}{kk'}g_1\right\} \\ &\quad+e\left(k'_\alpha-\frac{kk'}{k^2}k_\alpha\right)\left(k_\mu-\frac{kk'}{k'^2}k'_\mu\right)\frac{k'^2}{kk'}\{kk'g_0-g_1\}. \end{aligned} \tag{A10}$$

Notice that the contribution of the second Lorentz structure in (A10) vanishes both for $k^2=0$ [because of the constraint of Eq. (A7) at $k'^2=0$, $kp=kk'$] and for $k'^2=0$. However, it does not vanish for both $k^2,k'^2\neq 0$; therefore, the second Lorentz structure contributes to the amplitude of the four-lepton decays.

We can now build the bridge to the form factors which describe the real photon emission by the valence quarks defined in Eq. (2.6); denoting the momentum of the l^+l^- pair as q, i.e., setting $k^2=0$ and replacing $k'^2\to q^2$, we obtain the form factors in Eq. (2.6) through the form factors $g,a_2,g_2,g_1(k'^2=q^2,k^2=0)$,

$$\begin{aligned} F_V(q^2,0)&=2M_B g(q^2,0),\\ F_A(q^2,0)&=-M_B a_2(q^2,0), \end{aligned} \tag{A11}$$

$$F_{TV}(q^2,0)=-[g_2(q^2,0)+g_1(q^2,0)],$$

$$F_{TA}(q^2,0)=-\left[g_2(q^2,0)+\frac{M_B^2+q^2}{M_B^2-q^2}g_1(q^2,0)\right]. \tag{A12}$$

The form factors describing the real photon emission from the penguin, are obtained by setting $k'^2=0$ and replacing $k^2\to q^2$ in the form factors $g_{1,2}(k'^2,k^2)$,

$$F_{TV}(0,q^2)=F_{TA}(0,q^2)=-[g_2(0,q^2)+g_1(0,q^2)]. \tag{A13}$$

APPENDIX B: DERIVATION OF $H^{\rm NF}_{\mu\alpha}$

Here we provide the derivation of Eq. (3.13). Our starting point is the matrix element,

$$H_{\mu\alpha}(k',k)=i\int dz e^{ik'z}\langle 0|T\{eQ_c\bar c\gamma_\mu c(z),eQ_s\bar s\gamma_\alpha s(0)\}|B_s(p)\rangle,\qquad p=k'+k, \tag{B1}$$

where the quark operators are Heisenberg operators in the SM, i.e., the corresponding S-matrix includes weak and strong interactions. The nonfactorizable contribution is related to the octet-octet part of the weak Hamiltonian and requires the emission of at least one soft gluon from the charm-quark loop,

$$H^{\rm NF}_{\mu\alpha}(k',k)=i\int dz\, e^{ik'z}\langle 0|T\left\{\bar eQ_c c(z)\gamma_\mu c(z),i\int dy\, L^{b\to s\bar cc[8\times8]}_{\rm weak}(y),i\int dx\, L_{Gcc}(x),eQ_s\bar s(0)\gamma_\alpha s(0)\right\}|\bar B_s(p)\rangle. \tag{B2}$$

We place $L_{\rm weak}$ at $y=0$ by shifting coordinates of all operators through the translation $\mathcal{O}(x)=e^{i\hat Py}\mathcal{O}(x-y)e^{-iy\hat P}$. Using the relations $\langle 0|e^{i(\hat Py)}=\langle 0|$ and $e^{-i(y\hat P)}|B_s(p)\rangle=e^{-i(py)}|\bar B_s(p)\rangle$, and changing the variables $x-y\to x$, $z-y\to z$, $y\to -y$, we find

$$H^{\rm NF}_{\mu\alpha}(k',k)=i^3e^2Q_cQ_s\int dxdydz e^{ik'z+iky}\langle 0|T\{\bar c(z)\gamma_\mu c(z),L^{b\to s\bar cc[8\times8]}_{\rm weak}(0),L_{Gcc}(x),\bar s(y)\gamma_\eta s(y)\}|\bar B_s(p)\rangle. \tag{B3}$$

Taking into account that $L^{b\to s\bar cc[8\times8]}_{\rm weak}=-H^{b\to s\bar cc[8\times8]}_{\rm weak}$ [the latter given by Eq. (2.13)], we obtain

$$\begin{aligned} H^{\rm NF}_{\mu\alpha}(k',k)=&-2C_2\frac{G_F}{\sqrt2}V_{cb}V^*_{cs}e^2Q_cQ_s i\int dxdydz e^{ik'z+iky}\langle 0|T\{\bar c(z)\gamma_\mu c(z),\bar c(0)\gamma_\beta(1-\gamma_5)t^a c(0),\bar c(x)\gamma_\nu t^b c(x)|0\rangle \\ &\times\langle 0|T\{\bar s(y)\gamma_\alpha s(y),\bar s(0)\gamma_\beta(1-\gamma_5)t^a b(0),B^b_\nu(x)\}|\bar B_s(p)\rangle. \end{aligned} \tag{B4}$$

It is convenient to insert, under the integral (B4), the identity

$$B^b_\nu(x) = \frac{1}{(2\pi)^4}\int d\kappa dx' B^b_\nu(x') e^{i\kappa(x-x')}. \tag{B5}$$

This allows us to isolate the contribution of the charm-quark loop $\Gamma^{\beta\nu\mu(ab)}_{cc}(\kappa, q)$,

$$H^{\rm NF}_{\mu\alpha}(k',k) = -2C_2\frac{G_F}{\sqrt{2}}V_{cb}V^*_{cs}e^2Q_cQ_s\frac{i}{(2\pi)^4}\int dy e^{iky}d\kappa e^{-i\kappa x'}\langle 0|T\{\bar s(0)\gamma_\beta(1-\gamma_5)b(0), B^b_\nu(x'), \bar s(y)\gamma_\alpha s(y)\}|B_s(p)\rangle$$
$$\times \underbrace{\int dxdz e^{iqz+i\kappa x}\langle 0|T\{\bar c(z)\gamma_\mu c(z), \bar c(0)\gamma_\beta(1-\gamma_5)t^a c(0), \bar c(x)\gamma_\nu t^b c(x)\}|0\rangle}_{\Gamma^{\beta\nu\mu(ab)}_{cc}(\kappa,q)}. \tag{B6}$$

Using momentum representation for the s-quark propagator

$$\langle 0|T\{s(y)\bar s(0)\}|0\rangle = \frac{1}{(2\pi)^4 i}\int d\tilde k e^{-iky}\frac{\tilde k + m_s}{m_s^2 - \tilde k^2 - i0}, \tag{B7}$$

we obtain

$$H^{\rm NF}_{\mu\alpha}(k',k) = -2C_2\frac{G_F}{\sqrt{2}}V_{cb}V^*_{cs}e^2Q_cQ_s$$
$$\times \underbrace{\frac{1}{(2\pi)^8}\int d\tilde k dy e^{-i(k-q')y}dxd\kappa e^{-i\kappa x}\Gamma^{\beta\nu\mu(ab)}_{cc}(\kappa,q)\langle 0|\bar s(y)\gamma^\alpha\frac{\tilde k + m_s}{m_s^2-\tilde k^2}\gamma^\beta(1-\gamma^5)t^a B^b_\nu(x)b(0)|\bar B_s(p)\rangle}_{\bar H^{\rm NF}_{\mu\alpha}}. \tag{B8}$$

APPENDIX C: NUMERICAL RESULTS FOR THE FORM FACTORS $R_{A,V}(k'^2, k^2)$

We have calculated the form factors $R_i(k'^2, k^2)$ in the region $-5 < k^2(\mathrm{GeV}^2) < 0$ and $0 < k'^2(\mathrm{GeV}^2) < 4m_c^2$. However, calculations based on finite-order QCD diagrams cannot be trusted near quark thresholds (for instance, the calculated form factors exhibit steep rise at $k^2 \to 0$ which is unphysical, as the nearest meson pole lies at $k^2 = M_\phi^2$ and the two-meson threshold lies at $k^2 = 4M_K^2$). So we pursue the following strategy. We make use of the results of our calculation in the restricted rectangular region $-5 < k^2(\mathrm{GeV}^2) < -0.6$ and $0 < k'^2(\mathrm{GeV}^2) < 4$ (i.e., relatively far from quark thresholds) and interpolate them by a simple analytic formula which takes into account the presence of the poles at $k'^2 = M^2_{J/\psi}$ and $k^2 = M^2_\phi$. Numerical parameters in this formula are obtained by the fit in the mentioned restricted area.

For the form factors H_V and H_A we use the following fitting function:

$$R_{A,V}(y_1,y_2) = \frac{R_{00}}{(1-y_1)(1-y_2)(1-g_{11}y_1-g_{12}y_1^2)(1-(a_{20}+a_{21}y_1+a_{22}y_1^2)y_2+(b_{20}+b_{21}y_1+b_{22}y_1^2)y_2^2)},$$
$$y_1 \equiv k'^2/M^2_{J/\psi}, \qquad y_2 \equiv k^2/M^2_\phi. \tag{C1}$$

This formula takes into account the correct location of meson poles at $k'^2 = M^2_{J/\psi}$ and $k^2 = M^2_\phi$. The coefficients in this formula are obtained by interpolation in the region where our results may be trusted. The outcome of the fitting procedure is given in Table I.

TABLE I. Parameters in (C1) obtained by the interpolation of our numerical results for $R_{V,A}$.

	$R_{00}[\mathrm{GeV}^{-1}]$	g_{11}	g_{12}	a_{20}	a_{21}	a_{22}	b_{20}	b_{21}	b_{22}
R_V	400.4	−0.204	0.421	0.141	−0.041	−0.044	−0.026	0.006	0.005
R_A	398.0	−0.154	0.426	0.141	−0.063	−0.016	−0.026	0.010	0.001

APPENDIX D: NUMERICAL RESULTS FOR THE FORM FACTOR $F_{TV}(k'^2, k^2)$

The fit formula for the form factor $F_{TV}(k'^2, k^2)$ is obtained by a similar procedure as described in Appendix C:

(i) The numerical results for $F_{TV}(k'^2, k^2)$ are obtained by evaluating the formulas from Sec. 5B of [1] and the 2DAs $\phi_\pm$ given in Eqs. (5.11) and (5.12) of [1].

(ii) We use the numerical results in the range $0 < k'^2(\mathrm{GeV}^2) < 15$ and $-5 < k^2(\mathrm{GeV}^2) < -0.6$ [i.e., far below the quark thresholds located at $k'^2 = (m_b + m_s)^2$ and $k^2 = 4m_s^2$] and interpolate these numerical results using the analytic fit formula,

$$F_{TV}(y_1, y_2) = \frac{g_{00}}{(1-y_1)(1-y_2)(1-g_{11}y_1-g_{12}y_1^2)(1-(a_{20}+a_{21}y_1+a_{22}y_1^2)y_2+(b_{20}+b_{21}y_1+b_{22}y_1^2)y_2^2)},$$
$$y_1 \equiv k'^2/M_{B_s^*}^2, \qquad y_2 \equiv k^2/M_\phi^2. \tag{D1}$$

The analytic formula (D1) reflects the correct location of the physical poles at $k'^2 = M_{B_s^*}^2$ and $k^2 = M_\phi^2$. The fit parameters obtained by the interpolation procedure are summarized in Table II. The deviation between the fit formula and the results of the direct calculation are below 2% in the full range where the interpolation is made.

TABLE II. Parameters in (D1) obtained by the interpolation of our numerical results for F_{TV}.

	g_{00}	g_{11}	g_{12}	a_{20}	a_{21}	a_{22}	b_{20}	b_{21}	b_{22}
F_{TV}	0.152	−0.038	−0.129	−0.197	0.144	0.360	0.026	−0.021	−0.058

[1] I. Belov, A. Berezhnoy, and D. Melikhov, Charming-loop contributions in $B_s \to \gamma\gamma$ decay, Phys. Rev. D **108**, 094022 (2023).

[2] M. Beneke, G. Buchalla, M. Neubert, and C. T. Sachrajda, Penguins with charm and quark-hadron duality, Eur. Phys. J. C **61**, 439 (2009).

[3] M. Ciuchini, M. Fedele, E. Franco, A. Paul, and L. Silvestrini, Lessons from the $B^{0,+} \to K^{*0,+}\mu^+\mu^-$ angular analyses, Phys. Rev. D **103**, 015030 (2021).

[4] M. Ciuchini, M. Fedele, E. Franco, A. Paul, and L. Silvestrini, New physics without bias: Charming penguins and lepton universality violation in $b \to s\ell^+\ell^-$ decays, Eur. Phys. J. C **83**, 64 (2023).

[5] D. Guadagnoli, *B* discrepancies hold their ground, Symmetry **13**, 1999 (2021).

[6] M. Algueró, B. Capdevila, A. Crivellin, and J. Matias, Disentangling lepton flavour universal and lepton flavour universality violating effects in $b \to s\ell^+\ell^-$ transitions, Phys. Rev. D **105**, 113007 (2022).

[7] N. Gubernari, M. Reboud, D. van Dyk, and J. Virto, Improved theory predictions and global analysis of exclusive $b \to s\mu^+\mu^-$ processes, J. High Energy Phys. 09 (2022) 133.

[8] T. Hurth, F. Mahmoudi, D. Martinez Santos, and S. Neshatpour, Neutral current B-decay anomalies, Springer Proc. Phys. **292**, 11 (2023).

[9] A. Greljo, J. Salko, A. Smolkovic, and P. Stangl, Rare b decays meet high-mass Drell-Yan, J. High Energy Phys. 05 (2023) 087.

[10] M. Ciuchini, M. Fedele, E. Franco, A. Paul, and L. Silvestrini, Constraints on lepton universality violation from rare *B* decays, Phys. Rev. D **107**, 055036 (2023).

[11] D. Guadagnoli, C. Normand, S. Simula, and L. Vittorio, From $D_s \to \gamma$ in lattice QCD to $B_s \to \mu\mu\gamma$ at high q^2, J. High Energy Phys. 07 (**2023**) 112.

[12] D. Guadagnoli, C. Normand, S. Simula, and L. Vittorio, Insights on the current semi-leptonic *B*-decay discrepancies—and how $B_s \to \mu^+\mu^-\gamma$ can help, J. High Energy Phys. 10 (2023) 102.

[13] M. B. Voloshin, Large $O(m_c^{-2})$ nonperturbative correction to the inclusive rate of the decay $B \to X_s\gamma$, Phys. Lett. B **397**, 275 (1997).

[14] Z. Ligeti, L. Randall, and M. B. Wise, Comment on nonperturbative effects in $\bar{B} \to X_s\gamma$, Phys. Lett. B **402**, 178 (1997).

[15] G. Buchalla, G. Isidori, and S. J. Rey, Corrections of order $\Lambda_{\mathrm{QCD}}^2/m_c^2$ to inclusive rare *B* decays, Nucl. Phys. **B511**, 594 (1998).

[16] A. Khodjamirian, R. Ruckl, G. Stoll, and D. Wyler, QCD estimate of the long distance effect in $B \to K^*\gamma$, Phys. Lett. B **402**, 167 (1997).

[17] P. Ball and R. Zwicky, Time-dependent *CP* asymmetry in $B \to K^*\gamma$ as a (quasi) null test of the Standard Model, Phys. Lett. B **642**, 478 (2006).

[18] P. Ball, G. W. Jones, and R. Zwicky, $B \to V\gamma$ beyond QCD factorisation, Phys. Rev. D **75**, 054004 (2007).

[19] I. I. Balitsky, V. M. Braun, and A. V. Kolesnichenko, Radiative decay $\Sigma^+ \to p\gamma$ in quantum chromodynamics, Nucl. Phys. **B312**, 509 (1989).

[20] P. Ball and V. Braun, Higher twist distribution amplitudes of vector mesons in QCD: Twist—4 distributions and meson mass corrections, Nucl. Phys. **B543**, 201 (1999).

[21] P. Ball, Theoretical update of pseudoscalar meson distribution amplitudes of higher twist: The nonsinglet case, J. High Energy Phys. 01 (1999) 010.

[22] A. Khodjamirian, T. Mannel, A. Pivovarov, and Y.-M. Wang, Charm-loop effect in $B \to K^{(*)} l^+ l^-$ and $B \to K^* \gamma$, J. High Energy Phys. 09 (2010) 089.

[23] H. Kawamura, J. Kodaira, C.-F. Qiao, and K. Tanaka, B-meson light cone distribution amplitudes in the heavy quark limit, Phys. Lett. B **523**, 111 (2001); **536**, 344(E) (2002).

[24] V. Braun, Y. Ji, and A. Manashov, Higher-twist B-meson distribution amplitudes in HQET, J. High Energy Phys. 05 (2017) 022.

[25] V. M. Braun and I. Halperin, Soft contribution to the pion form-factor from light cone QCD sum rules, Phys. Lett. B **328**, 457 (1994).

[26] A. Khodjamirian, T. Mannel, and N. Offen, Form-factors from light-cone sum rules with B-meson distribution amplitudes, Phys. Rev. D **75**, 054013 (2007).

[27] N. Gubernari, D. van Dyk, and J. Virto, Non-local matrix elements in $B_{(s)} \to \{K^{(*)}, \phi\} \ell^+ \ell^-$, J. High Energy Phys. 02 (2021) 088.

[28] A. Kozachuk and D. Melikhov, Revisiting nonfactorizable charm-loop effects in exclusive FCNC B decays, Phys. Lett. B **786**, 378 (2018).

[29] D. Melikhov, Charming loops in exclusive rare FCNC B-decays, EPJ Web Conf. **222**, 01007 (2019).

[30] D. Melikhov, Nonfactorizable charming loops in FCNC B decay versus B-decay semileptonic form factors, Phys. Rev. D **106**, 054022 (2022).

[31] D. Melikhov, Three-particle distribution in the B meson and charm-quark loops in FCNC B decays, Phys. Rev. D **108**, 034007 (2023).

[32] Q. Qin, Yue-Long Shen, Chao Wang, and Yu-Ming Wang, Deciphering the long-distance penguin contribution to $\bar{B}_{d,s} \to \gamma\gamma$ decays, Phys. Rev. Lett. **131**, 091902 (2023).

[33] Y.-K. Huang, Y. Ji, Y.-L. Shen, C. Wang, Y.-M. Wang, and X.-C. Zhao, Renormalization-group evolution for the bottom-meson soft function, arXiv:2312.15439.

[34] B. Grinstein, M. J. Savage, and M. B. Wise, $B \to X(s) e^+ e^-$ in the six quark model, Nucl. Phys. **B319**, 271 (1989).

[35] A. J. Buras and M. Munz, Effective Hamiltonian for $B \to X(s) e^+ e^-$ beyond leading logarithms in the NDR and HV schemes, Phys. Rev. D **52**, 186 (1995).

[36] G. Buchalla, A. J. Buras, and M. E. Lautenbacher, Weak decays beyond leading logarithms, Rev. Mod. Phys. **68**, 1125 (1996).

[37] D. Melikhov, N. Nikitin, and S. Simula, Lepton asymmetries in exclusive $b \to s l^+ l^-$ decays as a test of the Standard Model, Phys. Lett. B **430**, 332 (1998).

[38] D. Melikhov, N. Nikitin, and S. Simula, Rare exclusive semileptonic $b \to s$ transitions in the Standard Model, Phys. Rev. D **57**, 6814 (1998).

[39] M. Beneke, C. Bobeth, and Y.-M. Wang, $B_{d,s} \to \gamma l^+ l^-$ decay with an energetic photon, J. High Energy Phys. 12 (2020) 148.

[40] D. Melikhov and N. Nikitin, Rare radiative leptonic decays $B_{d,s} \to \gamma l^+ l^-$, Phys. Rev. D **70**, 114028 (2004).

[41] F. Kruger and D. Melikhov, Gauge invariance and form-factors for the decay $B \to \gamma l^+ l^-$, Phys. Rev. D **67**, 034002 (2003).

[42] A. Kozachuk, D. Melikhov, and N. Nikitin, Rare FCNC radiative leptonic $B_{s,d} \to \gamma l^+ l^-$ decays in the Standard Model, Phys. Rev. D **97**, 053007 (2018).

[43] W. Lucha and D. Melikhov, The puzzle of the $\pi \to \gamma\gamma^*$ transition form factor, J. Phys. G **39**, 045003 (2012).

[44] C.-D. Lü, Y.-L. Shen, Y.-M. Wang, and Y.-B. Wei, QCD calculations of $B \to \pi, K$ form factors with higher-twist corrections, J. High Energy Phys. 01 (2019) 024.

[45] A. Khodjamirian, R. Mandal, and T. Mannel, Inverse moment of the B_s-meson distribution amplitude from QCD sum rule, J. High Energy Phys. 10 (2020) 043.

[46] P. Ball and E. Kou, $B \to \gamma e \nu$ transitions from QCD sum rules on the light cone, J. High Energy Phys. 04 (2003) 029.

[47] V. M. Braun, D. Yu. Ivanov, and G. P. Korchemsky, The B meson distribution amplitude in QCD, Phys. Rev. D **69**, 034014 (2004).

[48] M. Beneke and J. Rohrwild, B meson distribution amplitude from $B \to \gamma l \nu$, Eur. Phys. J. C **71**, 1818 (2011).

[49] Y. M. Wang, Factorization and dispersion relations for radiative leptonic B decay, J. High Energy Phys. 09 (2016) 159.

[50] Y. M. Wang and Y. L. Shen, Subleading-power corrections to the radiative leptonic $B \to \gamma \ell \nu$ decay in QCD, J. High Energy Phys. 05 (2018) 184.

[51] C. Wang, Y. M. Wang, and Y. B. Wei, QCD factorization for the four-body leptonic B-meson decays, J. High Energy Phys. 02 (2022) 141.

[52] T. Janowski, B. Pullin, and R. Zwicky, Charged and neutral $\bar{B}_{u,d,s} \to \gamma$ form factors from light cone sum rules at NLO, J. High Energy Phys. 12 (**2021**) 008.

[53] M. A. Ivanov and D. Melikhov, Theoretical analysis of the leptonic decay $B \to l l' \nu'$, Phys. Rev. D **105**, 014028 (2022); **106**, 119901(E) (2022).

[54] B. Y. Cui, Y. K. Huang, Y. L. Shen, C. Wang, and Y. M. Wang, Precision calculations of $B_{d,s} \to (\pi, K)$ decay form factors in soft-collinear effective theory, J. High Energy Phys. 03 (2023) 140.

[55] D. Melikhov and B. Stech, Weak form-factors for heavy meson decays: An update, Phys. Rev. D **62**, 014006 (2000).

[56] M. Beyer, D. Melikhov, N. Nikitin, and B. Stech, Weak annihilation in the rare radiative $B \to \rho\gamma$ decay, Phys. Rev. D **64**, 094006 (2001).

[57] A. Kozachuk, D. Melikhov, and N. Nikitin, Annihilation type rare radiative $B_{(s)} \to V\gamma$ decays, Phys. Rev. D **93**, 014015 (2016).

[58] C.-D. Lü, Yue-Long Shen, Chao Wang, and Yu-Ming Wang, Shedding new light on weak annihilation B-meson decays, Nucl. Phys. **B990**, 116175 (2023).

[59] Y.-K. Huang, Y.-L. Shen, C. Wang, and Y.-M. Wang, Next-to-leading-order weak annihilation correction to rare $B \to \{K, \pi\} \ell^+ \ell^-$ decays, arXiv:2403.11258.

[60] Max Ferre (private communication).